Kurdish Studies
August 2024
Volume: 12, No: 5, pp 897-915
ISSN: 2051-4883 (Print) | ISSN 2051-4891 (Online)
www.KurdishStudies.net

DOI: 10.53555/ks.v12i5.3373

Numerical Study Of Flow Behind The Tods In Side-By-Side Arrangement Through Lattice Boltzmann Method

Ali Ahmad[1], Raheela Manzoor[2*], Irfan Ali[3,4], Shazia Kalsoom[2], Noreen Azhar[2], Neelofer Jamil[5], Irum Javid[6], Farida Behlil[5]

[1]Department of Mathematics, University of Balochistan, Saryab road, Quetta, Balochistan, Pakistan.

[2*]Department of Mathematics, Sardar Bahadur Khan Women's University, Quetta, Balochistan, Pakistan

[3]Department of Mathematics: Analysis, Logic and Discrete Mathematics, Ghent University, 9000 Ghent, Belgium.

[4]Department of Mathematical Sciences, BUITEMS, Quetta 87300 Pakistan.

[5]Department of Chemistry, Sardar Bahadur Khan Women's University, Quetta, Balochistan, Pakistan

[6]Department of Biochemistry, Sardar Bahadur Khan Women's University, Quetta, Balochistan, Pakistan

***Corresponding Author:** Raheela Manzoor

*Email: raheela_manzoor@yahoo.com

ABSTRACT

A two-dimensional (2D) numerical analysis of flow past two and three square rods arranged side-by-side (SBS) using the numerical technique of the lattice Boltzmann method (LBM) is performed. The combined effects of gap spacing (g = g/D) for two rods and, in the case of three rods, the size (d/D) of the middle rod vary with the delay of vortex shedding. The flow across two and three square rods is examined for 0.5D ≤ g/D ≤ 4D and 0.1D ≤ d/D ≤ 1D at a fixed Reynolds number (Re = 160). The results indicate a strong correlation between middle rod size and flow characteristics for small gap spacings (g/D ≤ 1D). It is observed that at a large value of g/D and a small value of d/D, the secondary rod interaction frequency disappears, and the flow is fully controlled by the primary vortex shedding frequency. It is also observed that at g/D ≥ 1, the drag force for the upper and lower rods decreases with the addition of the middle rod. The observed flow regime (FR) without the middle rod (d/D = 0) is the irregular flow regime (FR), occurring at g/D = 0.5 and 1, and modulated antiphase synchronized FRs occur at g/D = 2, 3, and 4. In the presence of the middle rod, the irregular FR occurs at (g/D, d/D) = (0.5, 0.1 ≤ d/D ≤ 1) and (1, 0.1 ≤ d/D ≤ 0.8). While at (g/D, d/D) = (2, 0.1 ≤ d/D ≤ 0.6), (3, 0.1 ≤ d/D ≤ 0.6), and (4, 0.1 and 0.2), the modulated antiphase synchronized FR occurs in the presence of the middle rod.

Keywords: Lattice Boltzmann method, Square Rods, Gap spacing, Flow patterns, Reynolds number.

INTRODUCTION

The flow through multiple bluff bodies is of practical interest e.g. the flow around large buildings, tubes in heat exchangers, bridge piers, electrical poles, chimney, stacks and offshore platforms, etc. A number of studies have been taken for flow past bluff body arrays of different geometries (Kolar *et al.* (1997)). The flow interference effects strongly depend upon the bluff bodies' arrangement. One of the most typical arrangements is the SBS arrangement, where the bluff bodies face uniform flow. A number of studies have been taken place on two and three SBS circular rods (Sumnet *et al.* (1999), Guillaume *et al.* (1999) & Zhang and Zhou, (2001)). As compared to circular geometry, much less attention has been paid to the square geometry of the rods.

LITERATURE REVIEW

Agrawal *et al.* (2006) numerically analyzed the flow characteristics around two structures arranged in a cross flow direction and found the chaotic and synchronized patterns to Re = 73. Chiu and Ko, (1995) analyzed the mean static pressure distribution of two rods with 2:1 dimension ratio. They observed the bistable flows by varying g/D from 0.375 to 1.75. Further they found that the flow separates from the corners, whereas the formation of separation bubble depends on the critical separation of two rods. Ma *et al.* (2017) analyzed the different types of flow behaviors numerically behind two rods arranged as SBS at 16 ≤ Re ≤ 200 and 0 ≤ g/D ≤10.The researchers observed nine different flow regimes. Inoue *et al.* (2006) studied the sound generation mechanism behind the two structures arranged SBS numerically. Islam *et al.* (2016) examined three different types of flow characteristics for flow over three rods arranged SBS through Lattice Boltzmann method. Zdravkovich, (1968) analyzed the smoke visualization of the laminar wake behind three rods in various triangular arrangements. He observed the co-existence of multiple Karman vortex street. The vortices quickly disintegrated by forming a completely new single vortex street. Zheng, (2017) studied the flow behavior through three square rods (SC) at fixed Re = 150 and g/D = 1.1 – 9. They observed five different flow regimes for different ranges of g/D, namely; (i) based-bleed flow for g/D < 1.4; (ii) flip-flopping flow for 1.4 < g/D < 2.1; (iii) symmetrically biased beat flow for 1.2 < g/D < 2.6; (iv) non-biased beat flow for 2.6 < g/D < 7.25; and (v) weak interaction flow for $7.21 < g/D < 9$. Inoue and Suzuki, (2007) studied the sound effect of three SBS rods arranged at low Reynolds number values by using 2D unsteady compressible Navier-Stokes equations using the uniform flow. They observed that when the spacing is large, the flow interference is very weak and behaves like three separate rods flow. The frequency of vortex shedding remains the same, with the decrease in spacing. The flow interference plays a key rule, with the decrease in g/D the flow interference among the three rods become stronger and the vortex shedding from rods tends to synchronize. Burattini and Agrawal, (2013) analyzed three different kinds of FRs at $Re = 73$ and $0.5 \le g/D \le 6$. Kang, (2004) numerically analyzed the 2D flow through three circular rods arranged SBS at $Re = 100$ and $g/D < 5$and identified five different types of patterns. He also found that at $g/D < 1$, the middle structure drag coefficient is considerably lower than the drag values of the outer rods. Verma and Goverdhan, (2011) analyzed the flow features by using two circular rods arranged SBS arrangement for $Re = 200$.They found a repelling force between the rods. This repulsion force decreases as the g/D increases. Rahman *et al.* (2014) analyzed the various types of flow behavior and aerodynamic features of three rods arranged SBS. They observed that the flow transition is highly dependent on the spacing, particularly when there is unequal spacing. Wang and Zhou, (2005) experimentally analyzed the downstream flow characteristics of the two rods with SBS arrangement. They observed three different flow regimes, namely a single, asymmetrical and two coupled street flow regimes.

From the above-mentioned literature, it is clear that there are number of studies for flow past rods in SBS arrangement. However, to the best of our knowledge in open literature there is no study for the proposed problem. The primary aim of the present study is to control the flow and fluid forces. Furthermore, how the irregular wake structure mechanism can be controlled with the help of middle rod. In present paper, we will study the flow past two and three SCs with SBS arrangement. In case of three SCs, the size of outer rods are fixed while the size of middle rod is varied.

The other sections of the paper contain the description of the problem and boundary conditions, detail of numerical method, effect of computational domains, code validation, result and discussions and conclusions, organized in sections, 2, 3, 4, 5 and 6 respectively.

PROBLEM DESCRIPTION

The configuration of flow feature is shown in Fig. 1. A 2D numerical study is conducted to study the effect of g/D and middle rod of size d/D. The study is taken for fixed Reynolds number ($Re = 160$), while changing g/D from 0.5 to 4 and d/D from 0.1 to 1. C_l, C_m and C_u are the upstream, middle-stream and downstream rods, respectively. The size of outer rods is D that is fixed. The horizontal and vertical height of the channel are denoted by L_x and L_y, respectively. The upstream, downstream and vertical distances of the channel are $L_u = 8D$, $L_d = 25D$ and $L_y = 12D$, respectively. These values of upstream, downstream and vertical distances are selected after a careful investigation, so that the effect of boundary conditions at entrance and exit position can be reduced (Han *et al.* (2013). At the entrance position of flow, uniform inflow velocity is used, while the convective boundary condition is applied at the exit position of the channel, while at the upper and lower side of the channel periodic boundary conditions are applied (Guo *et al.* (2008)). At the surface of the rods no-slip boundary condition is applied (Zhou *et al.* (2009). All the fluid forces are calculated by using momentum exchange method (Yu *et al.* (2003).

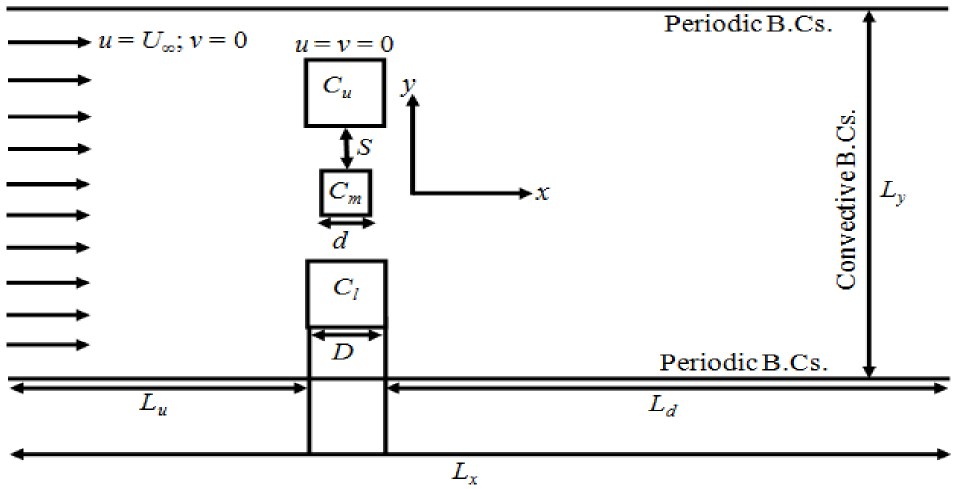

Figure 1 Configuration of flow past three square rods in an unconfined channel.

NUMERICAL METHOD (LBM)

A 2D Lattice Boltzmann code was established for this study. Because of low Reynolds number the two-dimensional assumption is used. As compared to other numerical scheme LBM is the latest numerical technique used to solve simple and complex flow problem. This numerical technique was developed by Frisch *et al.* (1986). A short description of this method is described here. A n_2m_9 model (where, n represents the dimension and m represents the particles number at a computational node) is used for the purpose of this work. In this model each node consists of eight moving particles and a rest particle at origin (Fig. 2). The Lattice Boltzmann equation is given by;

$$f_i(\mathbf{x} + \mathbf{e}_i, t+ 1) = f_i(\mathbf{x}, t) - [f_i(\mathbf{x}, t) - f_i^{(eq)}(\mathbf{x}, t)]/\tau. \quad (1)$$

where, f_i is distribution and $f_i^{(eq)}$ is equilibrium distribution function, $\mathbf{e}_i$ is the velocity component, t is the dimensionless time, $\mathbf{x}$ is the position of particles, and τ is single relaxation time. The equilibrium distribution function is described as:

$$f_i^{(eq)} = \rho\omega_i(1 + 3(\boldsymbol{e}_i.\boldsymbol{u}) + 4.5(\boldsymbol{e}_i.\boldsymbol{u})^2 - 1.5\boldsymbol{u}^2). \quad (2)$$

Here, $\boldsymbol{u}$ shows the instantaneous velocity of each node, ρ is the density of fluid and ω_i are the weighting coefficients. In n_2m_9, the weights for each node are as follows; $\omega_i = 9/4$ for the rest particle, $1/9$ for the particles 1 – 4, and $1/36$ for the particles 5 – 8.

Lattice Boltzmann method is based on two different steps: collision and streaming (Breuer *et al.* (2000), Sumner *et al.* (1999)). These steps can be mathematically expressed as:

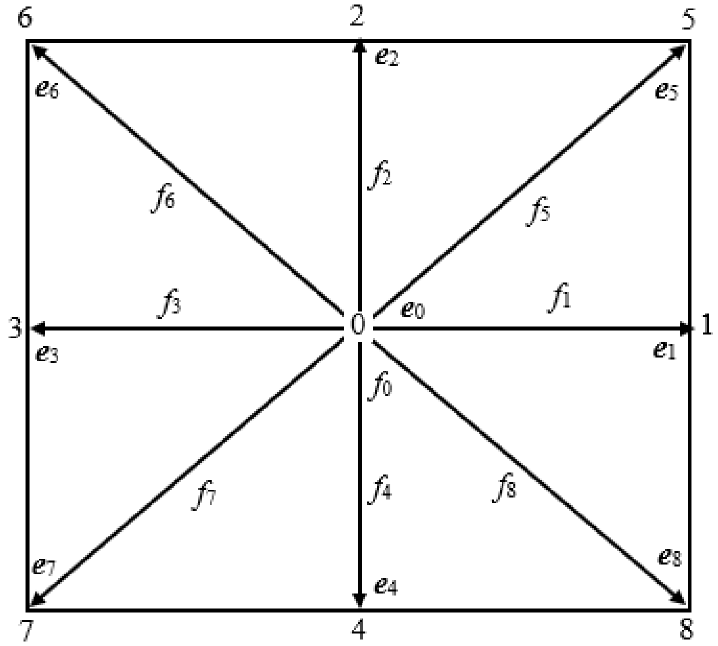

Figure 2 LBM lattice velocities on square structure.

Collision step: $f_i^{(new)}(\boldsymbol{x}, t) = f_i(\boldsymbol{x}, t) - [f_i(\boldsymbol{x}, t) - f_i^{(eq)}(x, t)]/\tau$. (3)

Streaming step: $f_i(\boldsymbol{x} + \boldsymbol{e}_i, t + 1) = f_i^{(new)}(\boldsymbol{x}, t)$. (4)

After the streaming step the boundary conditions are applied. To calculate the density and velocity we will use the following equations:

$$\rho = \sum_i f_i \quad (5)$$

$$\rho\boldsymbol{u} = \sum_i f_i\, \boldsymbol{e}_i \quad (6)$$

The pressure can be calculated from equation: $p = \rho c_s^2$; where c_s is the speed of sound and this equation is known as equation of state. It is to be noted that LBM has a second order accuracy in terms of space and time (Breuer *et al.* (2000)).

STUDY OF COMPUTATIONAL DOMAIN

The flow characteristics of flow around bluff bodies are strongly based on the size of the computational domain. The flow behavior totally changes, when there is a small change occurs in size of computation domain, and values of physical parameters are affected. In this section we have calculated the C_{Dmean} and St for different values of L_u, L_d, and L_y, so that we can choose a better computational domain. Table 1 is representing that there is a minute difference in between the resulted values of physical parameters. We will simulate the given problem by using $L_u = 8D$; $L_d = 25D$ and $L_y = 12D$.

Table 1 Effect of computational domain at g/D = 0.5 and d = 0.1.

L_u	L_d	L_y	C_{Dmeanl}	C_{Dmeanu}	St_l	St_u
8*D*	15*D*	12*D*	2.1957	2.2204	0.1543	0.1543
			(0.13%)	(0.54)%	0%	0%
8*D*	25*D*	12*D*	2.1929	2.2322	0.1543	0.1543
			(0.97%)	(0.21%)	0%	0%
8*D*	35*D*	12*D*	2.1717	2.2368	0.1543	0.1543
4*D*	25*D*	12*D*	2.2605	2.2837	0.158	0.158
			(3%)	(2.3%)	(2.4%)	(2.4%)
8*D*	25*D*	12*D*	2.1929	2.2322	0.1543	0.1543
			(2.5%)	(2.9%)	(3%)	(3%)

12*D*	25*D*	12*D*	2.1361	2.2.1689	0.159	0.159
8*D*	25*D*	6*D*	2.5123	2.5291	0.158	0.1740
			(2.6%)	(3%)	(2.4%)	(2.4%)
8*D*	25*D*	12*D*	2.1929	2.2322	0.1543	0.1543
			(2.9%)	(2.1%)	(3%)	(3%)
8*D*	25*D*	18*D*	2.1285	2.1843	0.1495	0.1495

CODE VALIDATION STUDY

The code validation is done against the problem of flow past a single SC at Re = 160. For validation, only two parameters are validated that are C_{Dmean} and St. The results of Chatterjee *et al.* (2009), Robichaux *et al.* (1999) and Sharma and Eswaran, (2004) are given in Table 2 for the comparison. The maximum deviation with data of Chatterjee *et al.* (2009)is 2.8% and 0.8% for C_{Dmean} and St, respectively. The maximum deviation with Robichaux *et al.* (1999) data is 3% for St. The maximum deviation with data of Sharma and Eswaran (2004) is 0.9% and 0% for C_{Dmean} and St, respectively. The results shows that the resulted C_{Dmean} and St are in correspond well with the numerical results of Chatterjee *et al.* (2009), Robichaux *et al.* (1999) and Sharma and Eswaran (2004)

Table 2 Comparison of present and previous numerical results.

	C_{Dmean}	St
Present	1.457	0.160
Chatterjee *et al.* (2009)	1.50	0.159
Robichaux *et al.* (1999)	-----	0.165
Sharma & Eswaran, (2004)	1.47	0.160

RESULTS AND DISCUSSIONS

We have conducted numerical simulations for flow past two and three SCs arranged SBS. In case of three SCs the size of upper and lower rods are fixed while the size of the middle rod is varied. The numerical simulations are carried out by varying the g/D and d/D size for a fixed Re = 160. The g/D will be varied from 0.5D to 4D and d/D varied from 0.1D to 1D. The results are studied in terms of instantaneous vorticity contours visualization, time histories of C_D and C_L, power spectra of C_L and force statistics analysis.

CHARACTERISTICS OF FLOW PAST TWO SIDE-BY-SIDE ARRANGED RODS

Firstly, we will discuss the various flow characteristics for two SBS rods in absence of middle rod. The irregular and modulated antiphase synchronized flow regimes are observed. Figure 3(a-c) presents the wake structure and its downstream evolution for different g/D values. At g/D = 1, there is reasonably enough space between the rods and the gap flow that effects the near wake downstream behind the rods. The lower and upper rods generate the wide and narrow wake, respectively. A similar flow behavior were found by Wang and Zhou[17] for flow over two circular rods. An increase in values of g/D, makes the gap flow and wakes interaction weaker, and the gap flow effect is almost insignificant.

At g/D = 2 and 4, the two rods wakes almost become synchronized, as presented in Figure 3(b, c). The streamline confirms that the vortex shedding pattern behind each rod occurs almost in the same phase, an alternate shed vortices move downward without any interaction with each other's (Figure 4(b, c)). Due to these characteristics, the FR is called the antiphase modulated synchronized flow regime. Such FR can also be found in the three circular rod flow by Kang, (2004) at g/D = 1.5 and Re = 100.

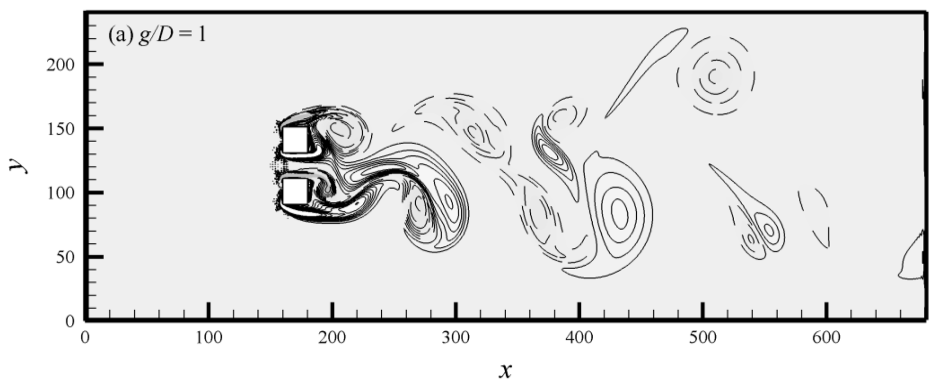

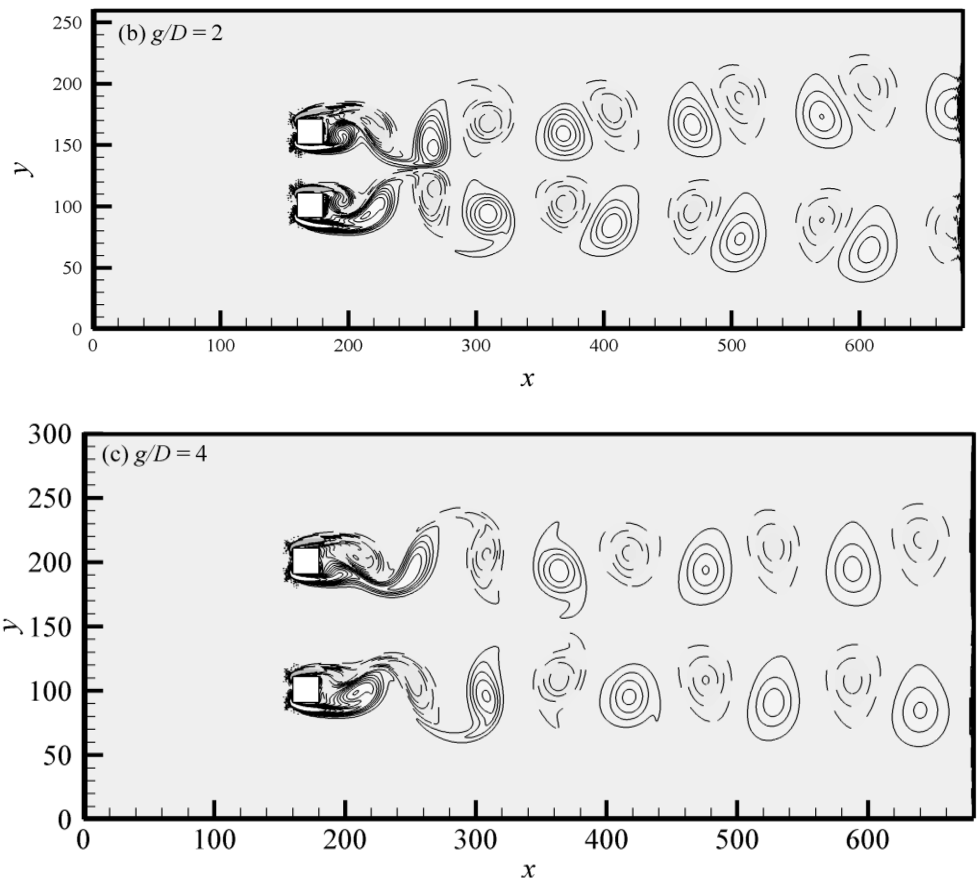

Figure 3(a-c). Flow regimes and its streamwise evolution at various spacing ratios.

Inspection of Figure 4(a-c) further confirms the existence of the irregular flow, and antiphase modulated synchronized flow regimes. In an irregular FR, the outer shear layers separated from the two rods merged with the gap flow near downstream of the rods, forming two smaller recirculation regions behind the lower rod and one recirculation region behind the upper rod (Figure 4(a)). Due to merging the forces are completely modulated. As seen in Figure 4(b, c), the influence of gap flow between the rods reduces with the increment in values of g/D. As a consequence, the modulated antiphase synchronized FR from the two rods are to be expected after a reasonably large spacing value of g/D (≥ 2).

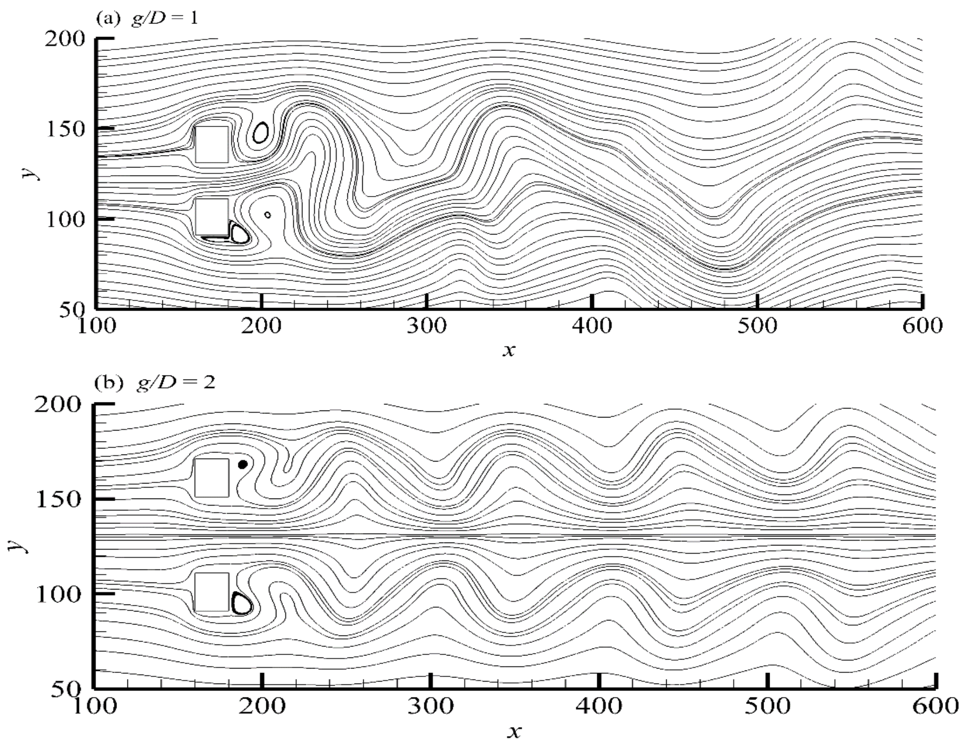

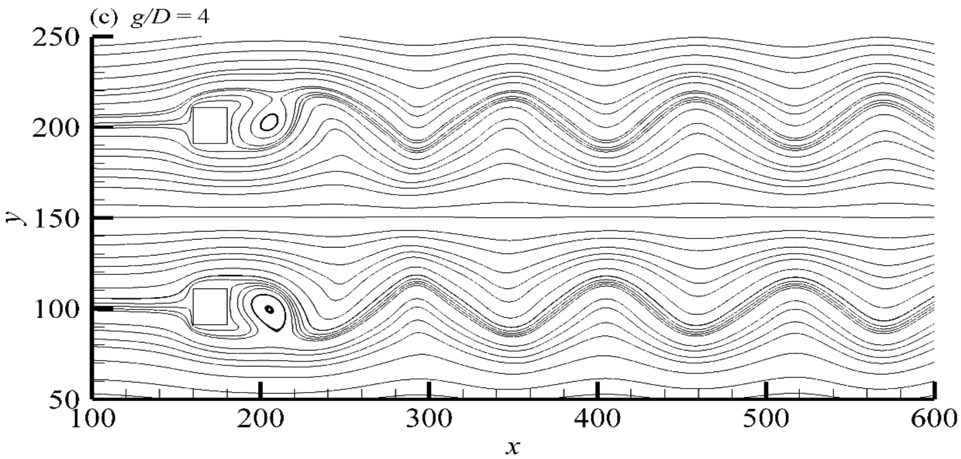

Figure 4(a-c) Visualization of streamlines for different flow regimes at different spacing values.

Time histories analysis of force coefficients are computed in order to investigate the influence of the g/D on the two SBS arranged rods. In order to examine the interaction of shed vortices quantitatively, the forces acting on the rods are computed. When the amplitude of two rods is same, then one can see the solid lines only in Figure 5(c, e). It is found that the generated shed vortices from the two rods are affected at $g/D = 1$. As a result, one can see the irregular variation of forces in Figure 5(a, b). At $g/D = 2$ and 4, lift coefficients becomes sinusoidal, and the outer rod shed vortices results in an antiphase mode (Figure 5(d, f)).

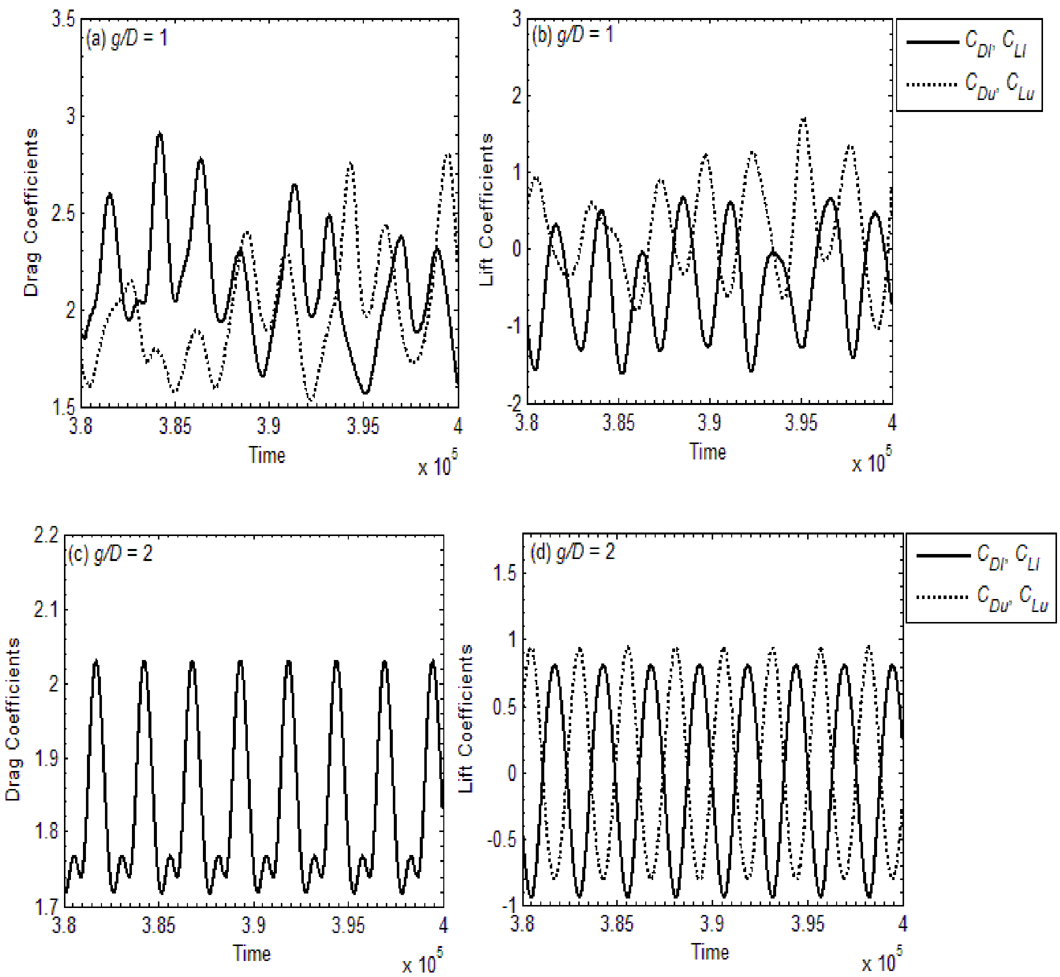

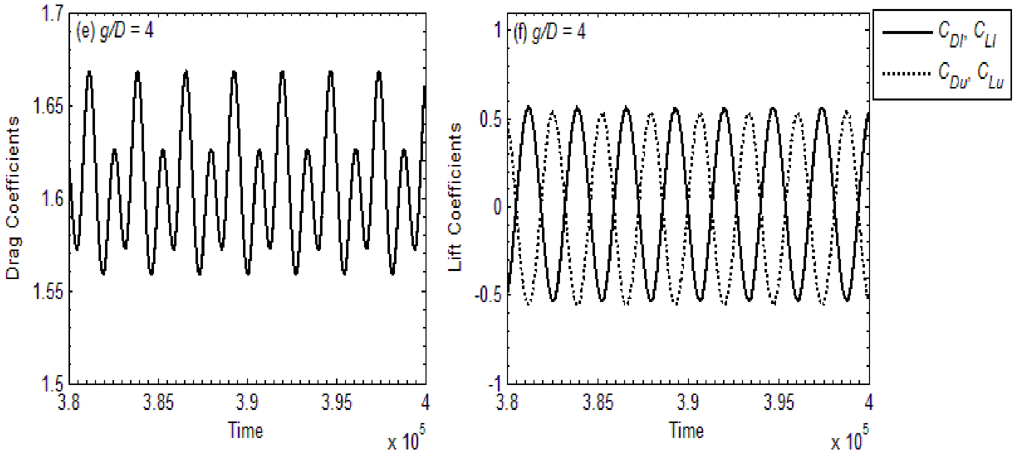

Figure 5(a-f) Time variation of C_D and C_L at different g/D.

The power spectra of C_L are calculated using the fast Fourier transform from which the vortex shedding frequency is extracted and presented in Figure 6(a-f). We will call the largest peak in the power spectra is primary frequency and the other peaks in the spectra will be called the secondary frequencies. The secondary frequencies confirm the continuous switching between narrow and wide wakes behind the two rods (Figure 6(a, b)). The power spectrum presented in Figure 6(c-f) confirms that in case of antiphase modulated synchronized FR, there is only one dominant shedding frequency for the two rods. At g/D = 2, a small peak in the power spectra suggests that the two rods flow is still affected by the gap flow but not seriously.

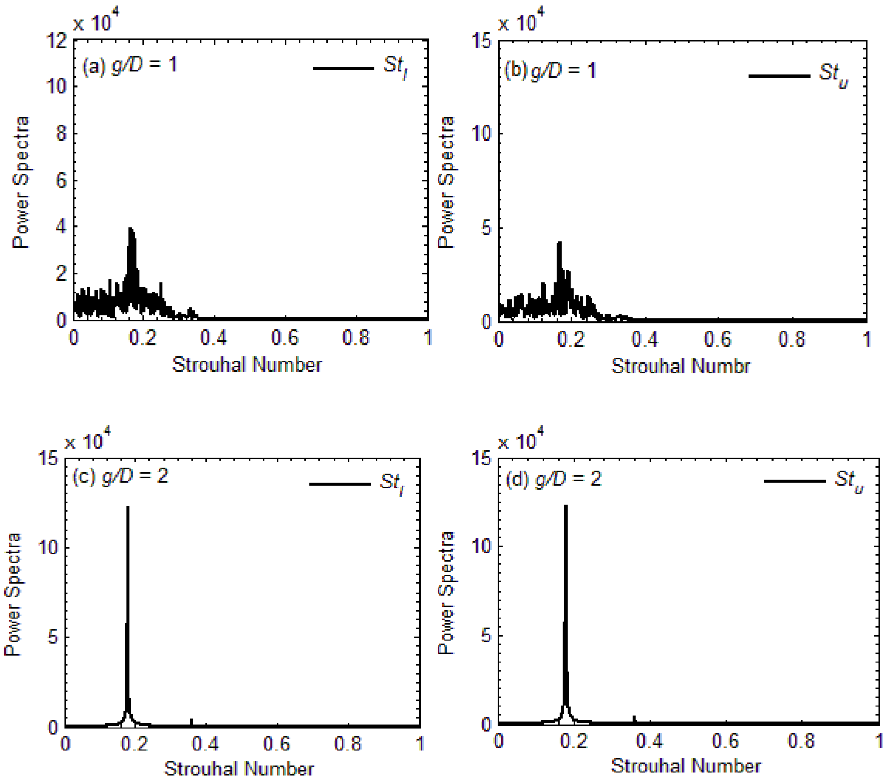

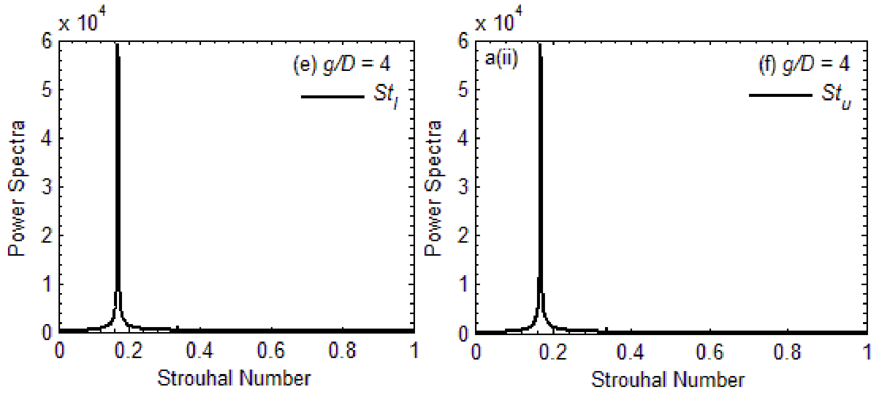

Figure 6(a-f). The spectra analysis of C_L at different g/D values.

The variation of the C_{Dmean}, St, C_{Drms} and C_{Lrms} with g/D values for two rods is presented in Table 3. The C_{Dmean} is found to decrease rapidly with an increase in gap spacing between the rods. At $g/D \geq 2$ where the gap flow may not affects the wake structure behind the two rods, and the Strouhal number of the C_l and C_u slowly decays from 0.1805 to 0.1674. This ensures that the rod C_l and C_u are behaving like an isolated rod at $g/D \geq 2$. The abrupt change in St, C_{Drms} and C_{Lrms} of two rods is found once the flow transition occurs from an irregular FR ($g/D = 1$) to modulated antiphase synchronized FR ($g/D \geq 2$).

Table 3 Variation of physical parameters as a function of g/D.

Gap spacing (g/D)	C_{Dmeanl}	C_{Dmeanu}	Stl	Stu
0.5	2.1147	2.1156	0.1368	0.1368
1.0	2.0052	2.0612	0.1642	0.1696
2.0	1.8338	1.8338	0.1805	0.1805
3.0	1.6900	1.6900	0.1740	0.1740
4.0	1.6065	1.6065	0.1674	0.1674
Spacing ratio (g/D)	C_{Drmsl}	C_{Drmsu}	C_{Lrmsl}	C_{Lrmsu}
0.5	0.2035	0.2106	0.3250	0.3301
1.0	0.2991	0.3116	0.5828	0.6068
2.0	0.1071	0.1071	0.6198	0.6198
3.0	0.0497	0.0497	0.4643	0.4643
4.0	0.0324	0.0324	0.3860	0.3860

THE EFFECT OF MIDDLE CONTROL ROD BETWEEN THE TWO RODS

It can be seen in Figure 7(a), that how the wake structure changes behind the lower and upper rods in presence of small rod in the middle of two SBS rods. The positive and negative vortex shedding from the lower and upper rods, respectively are observed in the flow field. One can find the required justification from the streamline visualization presented in Figure 9(a). Figure 9(a, b) represents the drag and lift coefficients for $g/D = 0.5$ and $d/D = 0.2$. A modulated sinusoidal variation is observed for the outer rods in presence of middle rod. This modulated frequency is due to the secondary frequencies produced by the two gap flows between the rods along with the primary frequency lead to multiple peaks observed in the power spectra of lift coefficients (ref. spectrum in Figure 10(a-c)).

The irregular FR is seen for the case with $g/D = 1$ and $d/D = 0.2$ in Figure 7(b). The vortices behind the downstream of the rods are not quite clear. Furthermore, the vortices from the outer rods are wider and narrower from the middle rod. In this FR, the gap flows are found to interact with each other's behind the rods. Such type of flow behavior was reported in the previous numerical study of Kang [14] for flow past circular rods at $Re = 100$. Figure 8(b) reconfirms that the irregular vortex shedding occurs behind the three SBS rods. The higher drag amplitudes observed for the outer rods as compared to the middle rod (Figure 9(c)). It is found that the lift coefficients for the outer rods are in-phase (Figure 9(d)).

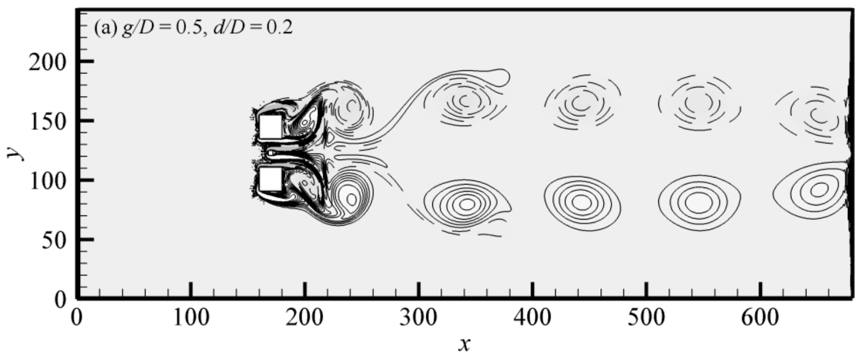

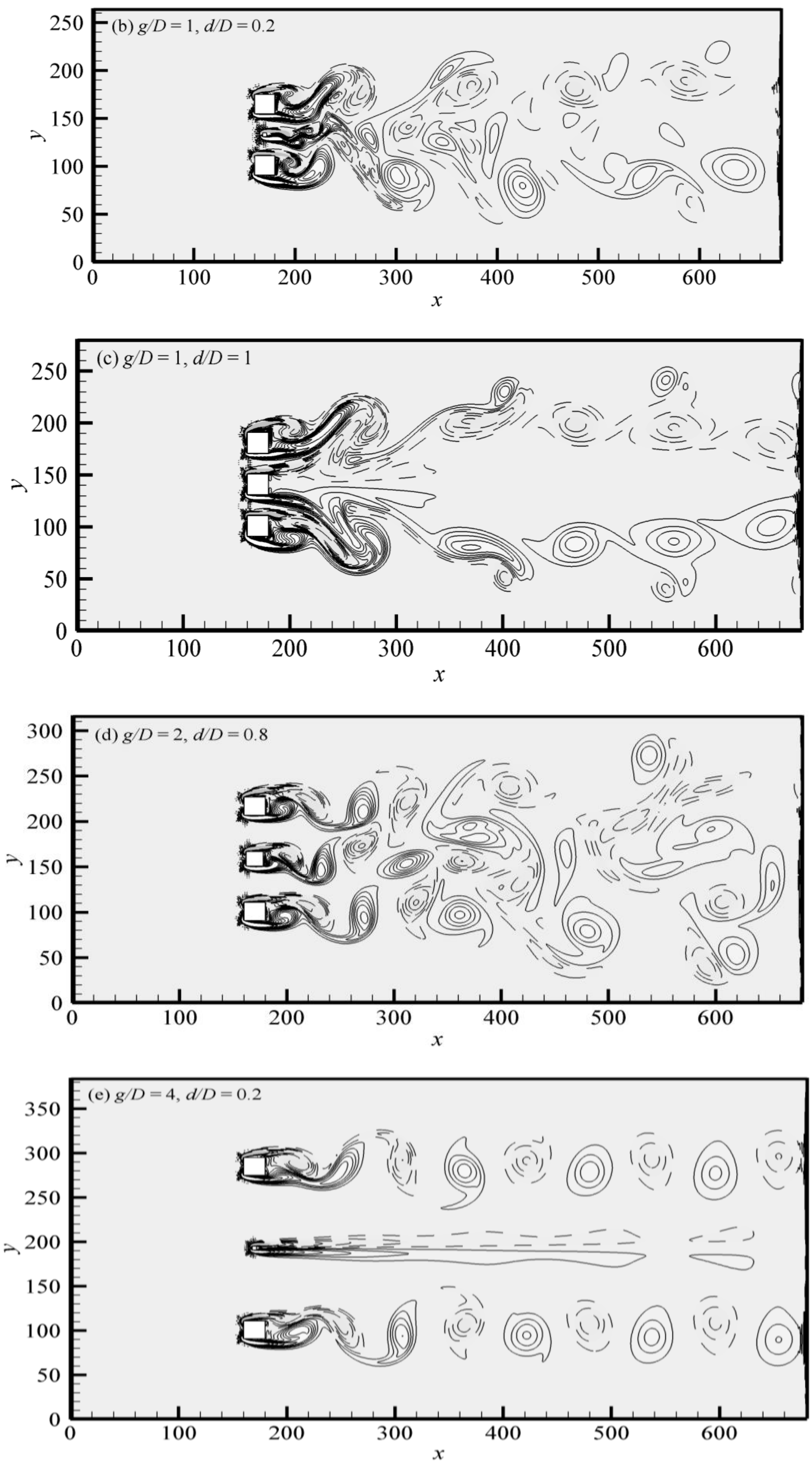
(b) g/D = 1, d/D = 0.2
(c) g/D = 1, d/D = 1
(d) g/D = 2, d/D = 0.8
(e) g/D = 4, d/D = 0.2
x
y

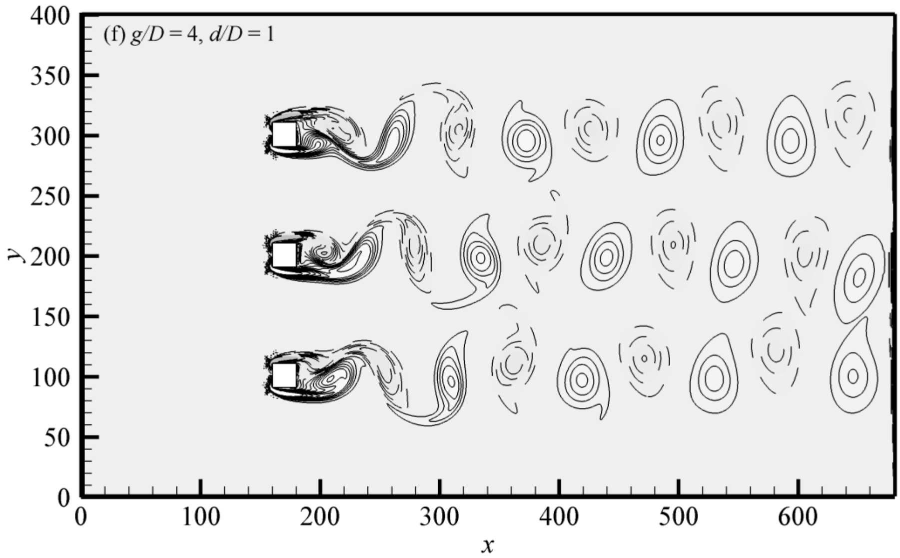

Figure 7(a-f) Flow regimes and its variation in streamwise direction at various g/D values.

In case of g/D = 1 (without middle rod), the forces of the outer rods are irregular (see Figure 5(a, b)). The power spectrum presented in Figure 10(d-f) was obtained by fast Fourier transform based on the time series analysis of the lift coefficients. It is found that there are multiple peaks in the spectra. As compared to the power spectra of two rods presented in Figure 6(a, b) the less peaks are observed in case of middle rod. As seen in Figure 7(c), the flow transition occurs with the increase of d/D value for the middle rod from 0.2 (irregular FR) to 1 (symmetric FR) at the same spacing (g/D = 1).

The streamline visualization of the three rods in Figure 8(c) shows some interesting flow behavior behind the rods. It is found that there exists one small circulation region on the lower surface and upper surface of the lower and upper rods, respectively. As a result, the negative and positive vortices shed in the form of two-row vortex-street from the upper and lower rods considerably different in terms of width and length as compared to the case presented in Figure 8(a). Interestingly the same drag value is observed for all three rods without any modulation (see Figure 9(e)). Due to the same value, one can only see the solid line in Figure 9(e). The lift force oscillation of the lower and upper rods was stable, which ensures that the influence of gap flows was almost negligible. The power spectra of lift coefficients of the three rods are shown in Figure 10(g-i). No Strouhal value for the middle rod is observed due to constant behavior of lift coefficient (Figure 10(i)). The spectra of the outer rods show only single dominant peak which suggest that only primary frequency have been observed.

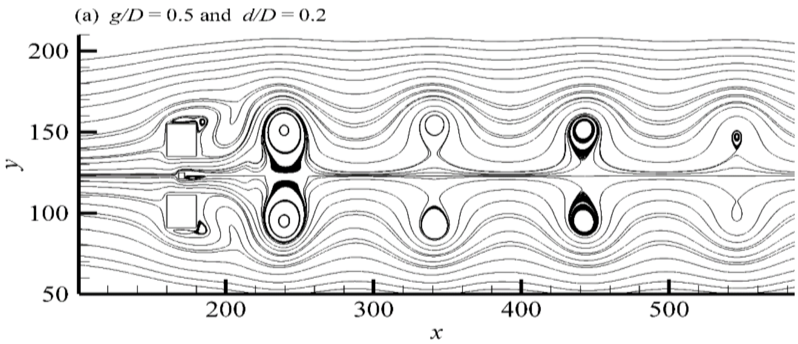

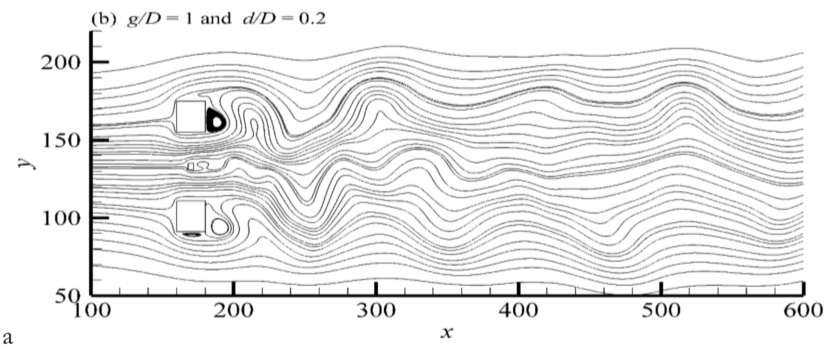

a

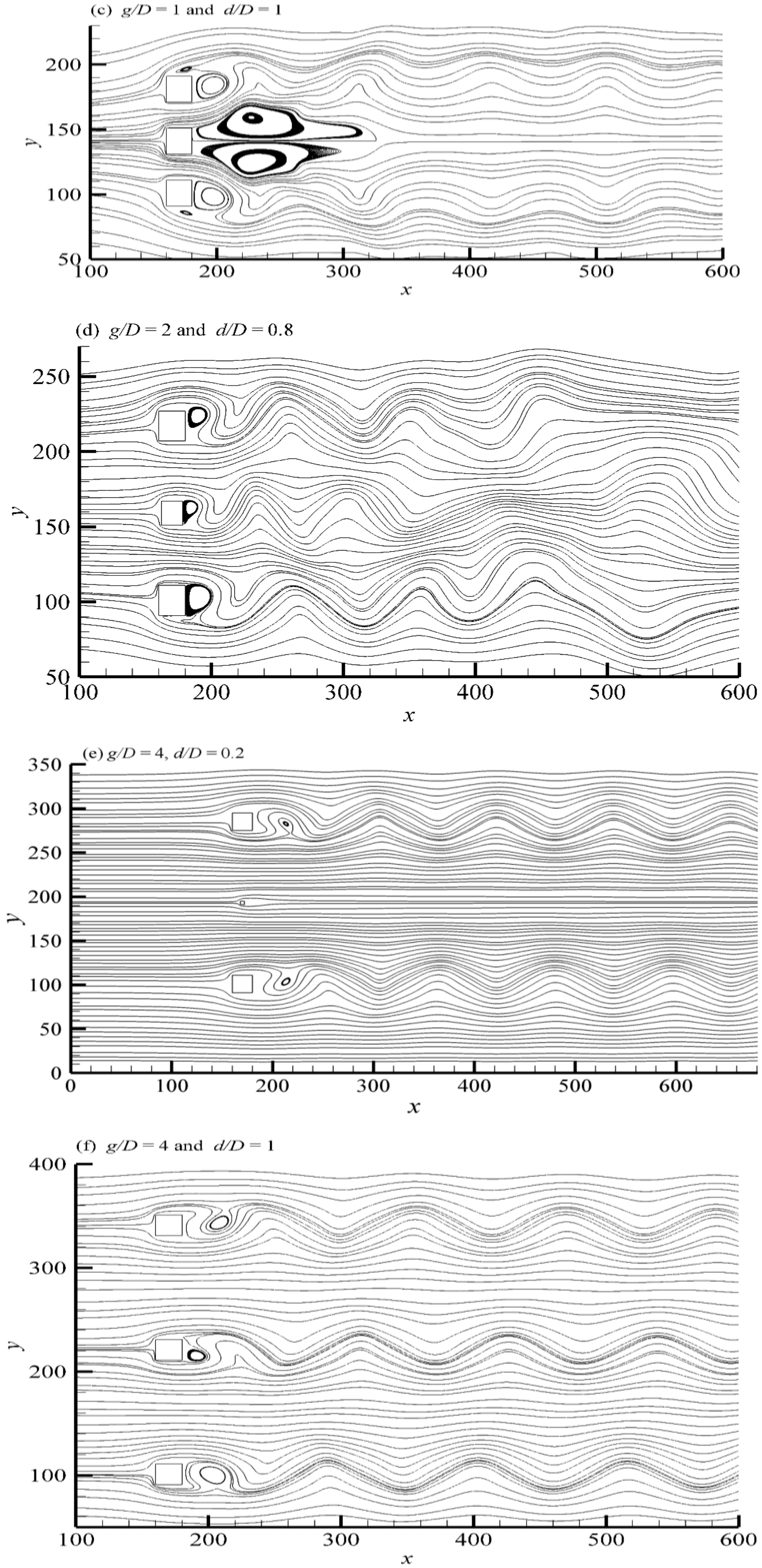

Figure 8(a-f) Visualization of streamlines for different flow regimes at different spacing values.

At (g/D, d/D) = (2, 0.8), the three rods wakes almost become synchronized, as presented in Figure 7(d). The vortex pattern behind each rod occurs almost in the same phase, alternate shed vortices move downward and shows some interaction with each other's. The slightly higher drag amplitude is observed for the lower rod as compared to the middle and upper rods (Figure 9(g)). Due to vortices interaction small modulation are also observed for the drag coefficients. It is observed from the streamline visualization that the vortex shedding processes behind the rods are independent presented in Figure 8(d). Inspection of Figure 9(h) further confirms that the flows behind the rods moves independently. The interaction of shed vortices with each other's at far downstream of the flow domain results in multi-frequency variation in the power spectrum of the lift coefficients of the three rods (ref. spectrum in Figure 10(j-l)).

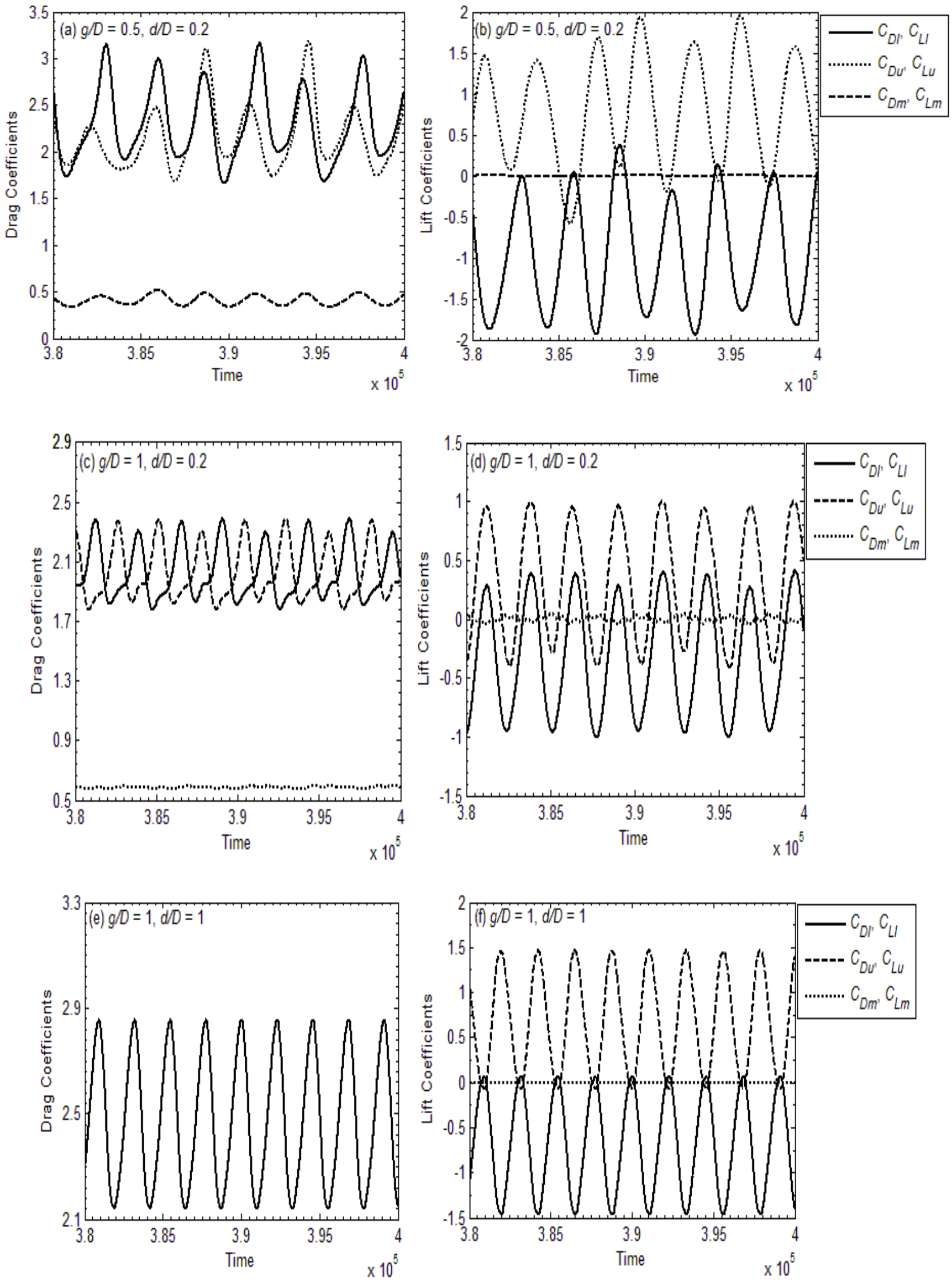

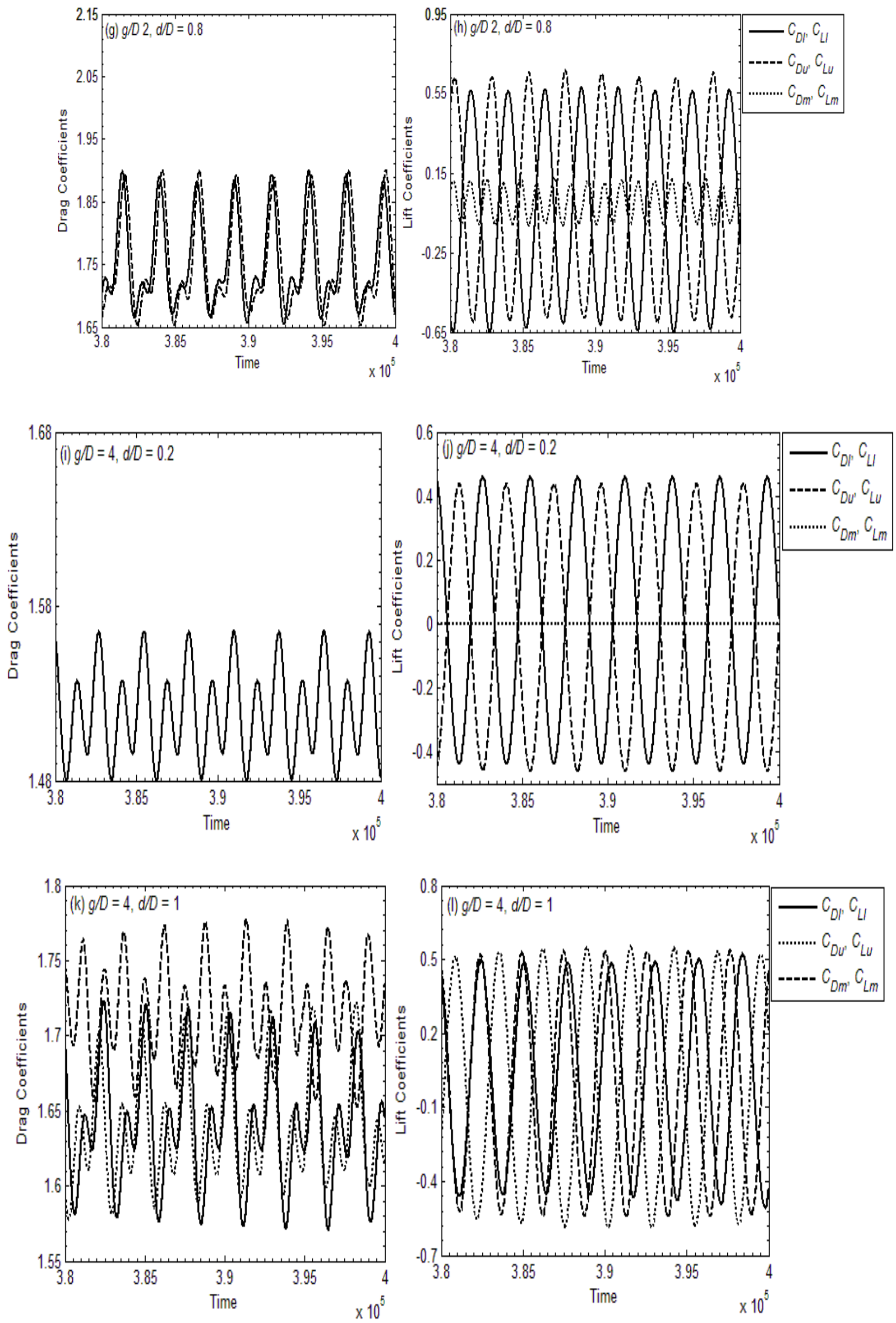

Figure 9(a-l) Time variation of forces at different *g/D* and *d/D* values.

The vorticity contours for g/D = 4 and d/D = 0.4 is presented in Figure 7I. The flow is symmetric behind the middle rod, while the flow behind the outer rods is antiphase. Such kind of flow behavior were also numerically observed by Han *et al.*[18] and experimentally by Zhang and Zhou[4] for g/D = 1.5. The wide wake is observed behind the middle rod. In streamline visualization graph presented in Figure 8I no recirculation region can be seen behind the middle rod due to symmetric nature. Upon increasing the size of the middle rod to d/D = 1, the vortex shedding mechanism is observed behind the middle rod (Figure 7(f)). It is quite clear from Figure 7(e, f) that the size of the middle rod plays a major role in the stability of flow behind the two rods, compared to the absence, of the middle rod. Figure 7(f) reconfirms that the vortex shedding occurs from the middle SC. It is also observed that the vortex shedding process of the lower and upper rods to be independent of the middle rod due to reasonably large g/D value between the rods. Inspection of Figure 9(I, j, k, l) further confirms that the flow behind the outer rods to be independent of the middle rod. From Figure 10(n-s), it is seen that the spectra analysis are changed while changing the size of the middle rod.

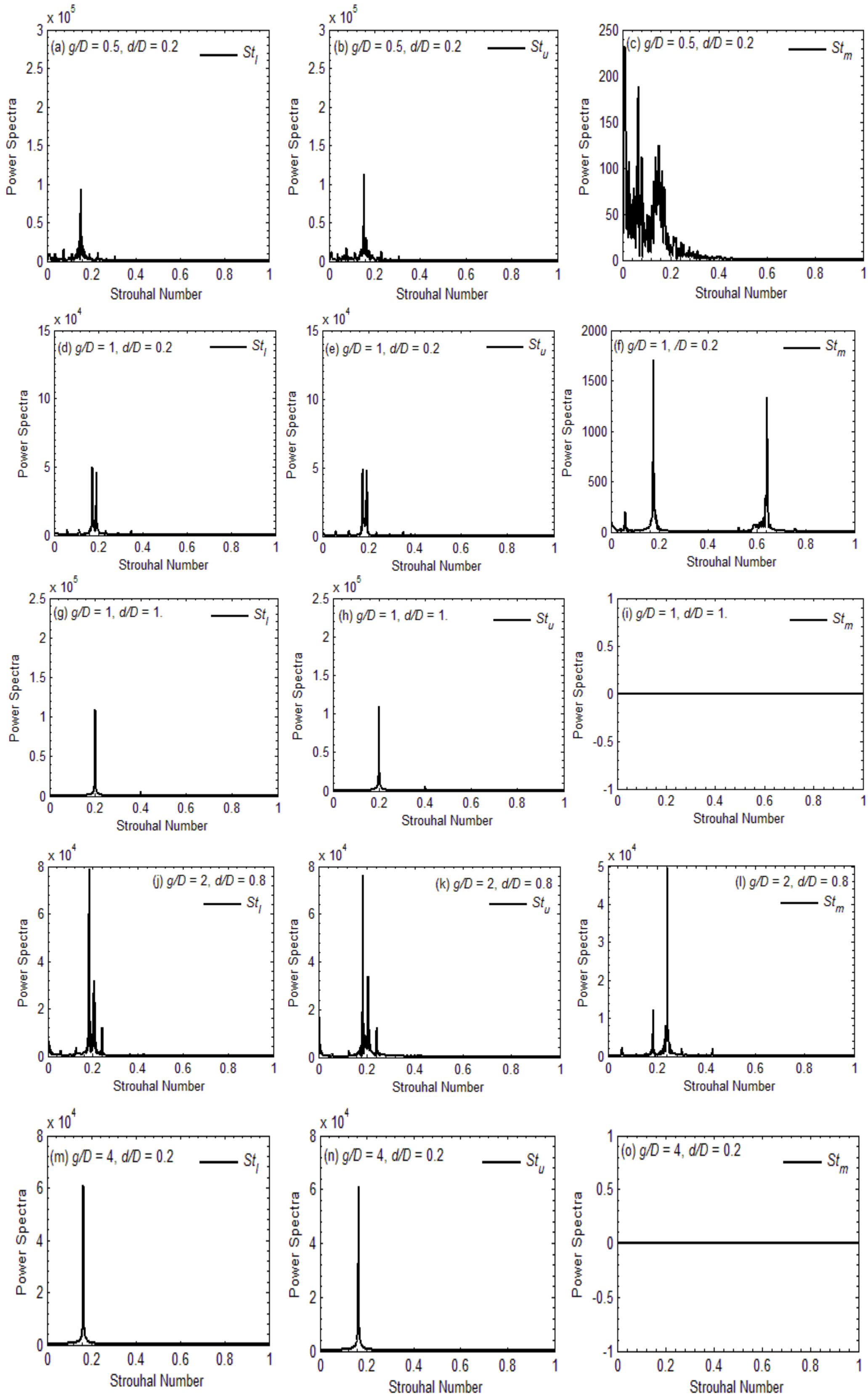
(a) g/D = 0.5, d/D = 0.2
St_l
(b) g/D = 0.5, d/D = 0.2
St_u
(c) g/D = 0.5, d/D = 0.2
St_m
(d) g/D = 1, d/D = 0.2
St_l
(e) g/D = 1, d/D = 0.2
St_u
(f) g/D = 1, /D = 0.2
St_m
(g) g/D = 1, d/D = 1.
St_l
(h) g/D = 1, d/D = 1.
St_u
(i) g/D = 1, d/D = 1.
St_m
(j) g/D = 2, d/D = 0.8
St_l
(k) g/D = 2, d/D = 0.8
St_u
(l) g/D = 2, d/D = 0.8
St_m
(m) g/D = 4, d/D = 0.2
St_l
(n) g/D = 4, d/D = 0.2
St_u
(o) g/D = 4, d/D = 0.2
St_m
Power Spectra
Strouhal Number

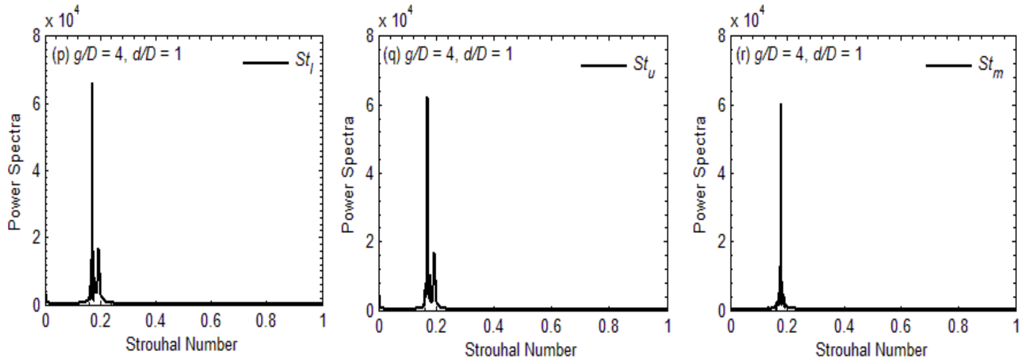

Figure 10(a-s) Power spectra analysis of C_L at various g/D values.

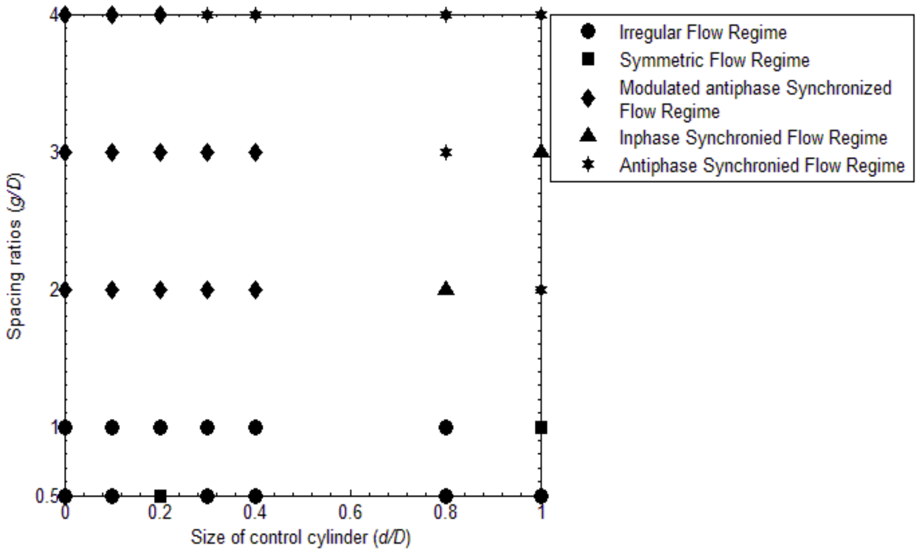

Figure 11 Flow regime diagram at various g/D and d/D values.

The graphical representation of various flow regimes, observed in this study, is given in Figure 11 at selected values of g/D and d/D. It can be observed that without middle rod (d/D = 0) the irregular FR occurs at g/D = 0.5 and 1 and modulated antiphase synchronized FR occurs at g/D = 2, 3, and 4. In presence of middle rod the irregular FR occurs at (g/D, d/D) = (0.5, 0.1 ≤ d/D≤ 1) and (1, 0.1 ≤ d/D≤ 0.8). While at (g/D, d/D) = (2, 0.1 ≤ d/D ≤ 0.6), (3, 0.1 ≤ d/D ≤ 0.6) and (4, 0.1 and 0.2) the modulated antiphase synchronized FR occurs in presence of middle rod. It can be seen from the figure that at (g/D, d/D) = (0.5, 0.2) and (1, 1) the symmetric FR occurs. At (g/D, d/D) = (2, 0.8) and (3, 1) the inphase synchronized FR occurs. The antiphase-inphase synchronized FR occurs at (g/D, d/D) = (2, 1), (3, 0.8) and (4, 0.6 ≤ d/D ≤ 1). For the purpose of comparison, the C_{Dmean}, St, C_{Drms} and C_{Lrms} on a single rod for different is also plotted in Figures 12(a-e) to 15(a-e). It is observed that the mean drag coefficient of the middle rod is smaller than the outer rods values. Slightly higher than the outer rods at g/D = 0.5 and 1 and d/D = 1. It can be seen from Figure 12(a-e) that the C_{Dmeanm} is more sensitive for the smaller middle rod size (d/D = 0.1 to 0.4). The mean drag coefficient of the middle rod increases as size of the middle rod increases. As the size of the middle rod increased, the C_{Dmean} of the outer rods slightly changed and was higher to that of a isolated rod for g/D = 0.5, 1, 2 and 4. The C_{Dmean} of the middle rod was smaller than that of the isolated one. When the value of middle rod increased to 0.8, the C_{Dmean} of the middle rod becomes equal or higher than that of a isolated rod. At higher separation ratio the C_{Dmean} of three rods almost equal and slightly higher than the isolated rod case (C_{Dmean} = 1.470). The mean drag coefficient of the middle rod quickly increases for the d/D values where FR transitions were observed.

As the size of the middle rod increased, the St value approached to the value obtained from a flow past a single rod (Figure 13(a-e)). On the other hand, the vortex shedding frequency for outer rods was unaffected and almost approaches to the value of an isolated rod. The middle rod Strouhal value is slightly affected as compared to the lower and upper SC value. Interestingly, for all d/D values, the lower rod and upper rod Strouhal values are almost equal to the Strouhal value of flow past an isolated rod (St = 0.1591). At g/D = 0.5, the middle rod Strouhal value (Stm) is lower than the isolated rod value. Furthermore, at g/D ≥ 2, the Strouhal value of the middle rod is slightly higher than the isolated rod value. The reason is that at large g/D value the shed vortices from the rods are move independently without any serious interaction in the far wake region downstream of the rods.

Figure 14(a-e) shows the variation of the C_{Drms} with the d/D for Re = 160. The middle rod has a maximum C_{Drms} value at d/D = 1 for all spacing ratios. The C_{Drms} of the middle rod is much larger than that of the isolated rod for 0.6 ≤ d ≤ 1 for all selected range of g/D. At 0.1 ≤ d/D ≤ 0.5, the C_{Drms} of the middle rod is almost approaches to that of an isolated rod. The C_{Lrms} value of the middle rod C_m is lower than that of an isolated rod except at the g/D = 2 to 4 and d/D = 1 where C_{Lrmsm} is nearly equal to the C_{Lrms} value of an isolated rod. It can be seen that the C_{Lrms} on the middle rod is sensitive to g/D and d/D, while those on the outer rods is not too much sensitive. The C_{Lrms} of the outer rods was almost equal to that of an isolated rod in case of g/D = 3 and 4 for all selected range of size of middle rod. It is found that the C_{Lrms} of the lower and upper rods were too close. It is observed that the outer rod was less affected by the middle rod when $g/D \geq 3$ (Figure 15(d, e)).

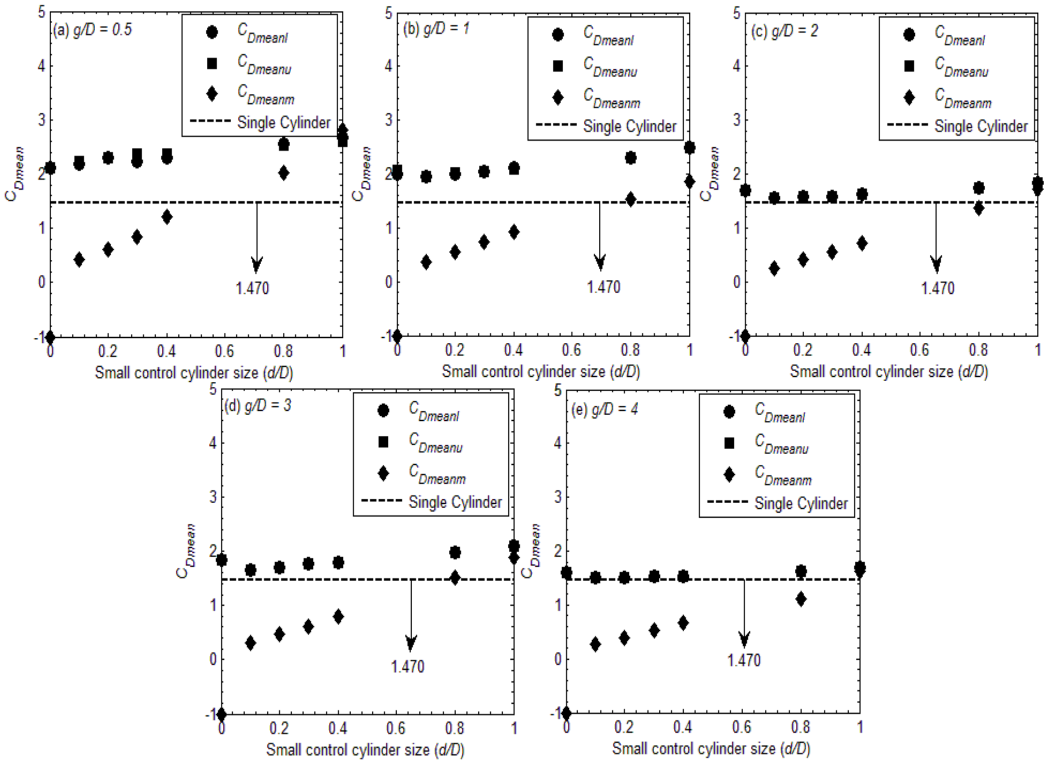

Figure 12(a-e) Variation of C_{Dmean} as a function of d/D.

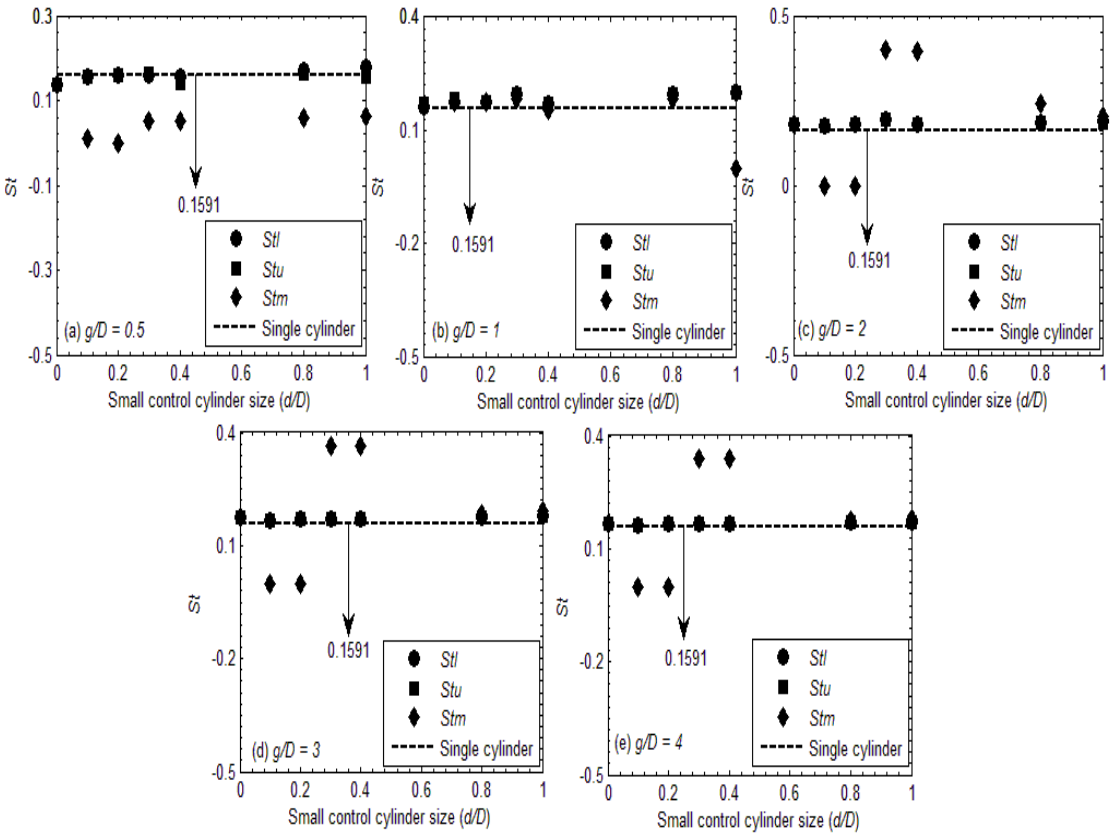

Figure 13(a-e). Variation of St as a function of d/D.

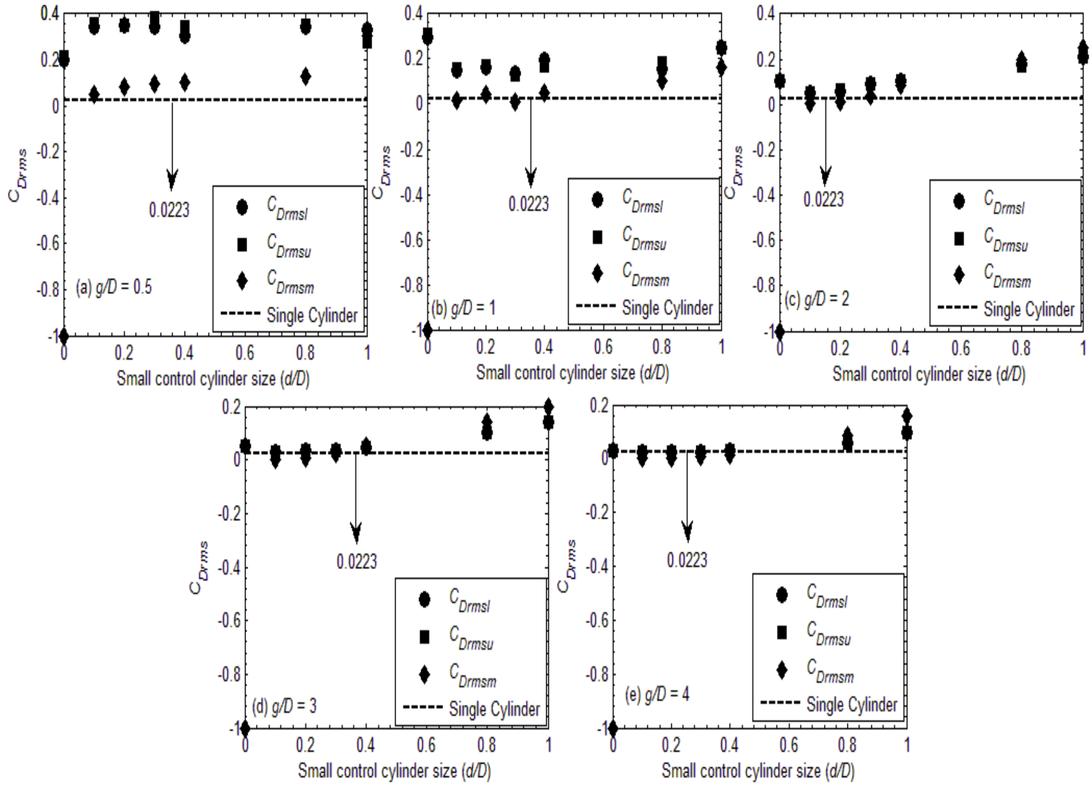

Figure 14(a-e) Variation of C_{Drms} as a function of d/D.

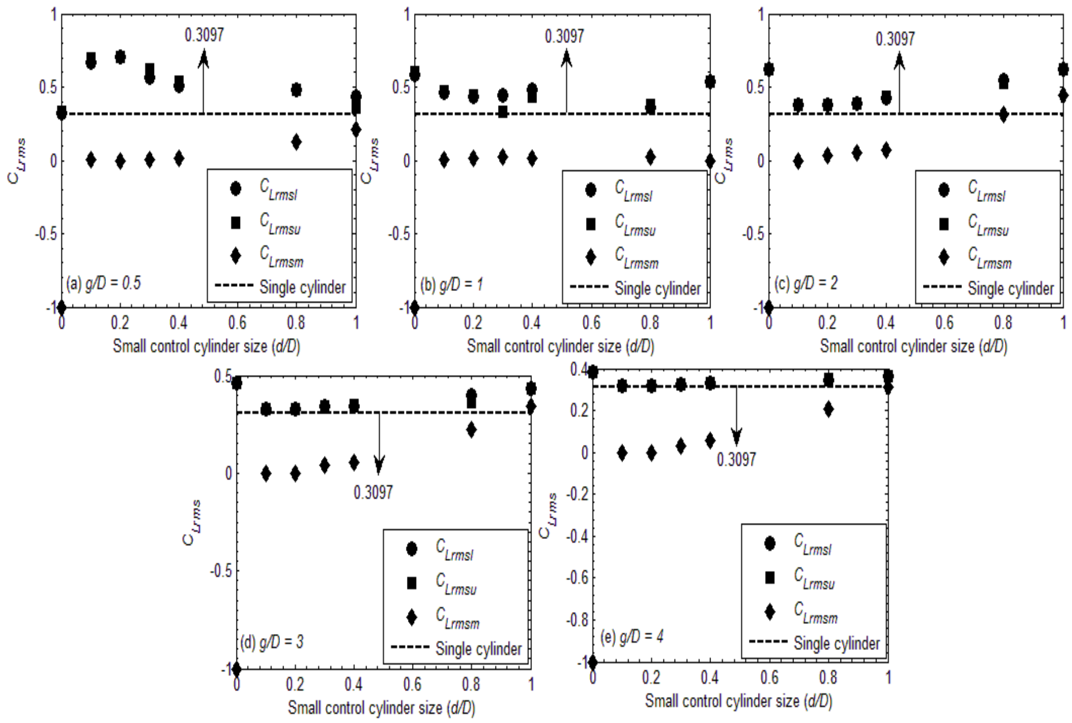

Figure 15 Variation of C_{Lrms} as a function of d/D.

CONCLUSIONS

In this chapter, we have numerically analyzed flow past over two and three rods. For the investigation, numerical simulations were performed, on the flow past rods in the range of $g/D = 0.5$ to 4 and $d/D = 0.1$ to 1 at $Re = 160$. It is found that without middle rod ($d/D = 0$) as gap spacing increases an irregular FR occurs at $g/D = 0.5$ and 1 and modulated antiphase synchronized FRs occurs at $g/D = 2$, 3, and 4. In presence of middle rod the irregular FR occurs at (g/D, d/D) = (0.5, $0.1 \le d/D \le 1$) and (1, $0.1 \le d/D \le 0.8$). While at (g/D, d/D) = (2, $0.1 \le d/D \le 0.6$), (3, $0.1 \le d/D \le 0.6$) and (4, 0.1 and 0.2) the modulated antiphase synchronized FR occurs in presence of middle rod. It is found that the flow is symmetric behind the middle rod at $g/D = 4$ and $d/D = 0.4$, while the flow behind the lower and upper rods are antiphase. The wide wake is observed behind the middle rod. The secondary frequencies confirm the continuous switching between narrow and wide wakes behind the rods in case of irregular FR. The abrupt change in St, C_{Drms} and C_{Lrms} of two rods is found once the flow transition occurs from irregular FR (g/D = 1) to modulated antiphase synchronized FR ($g/D \geq 2$). The study found that the presence of a middle rod significantly influenced the forces exerted on the rods and the frequency of vortex shedding. Abrupt changes in these parameters coincided with transitions between flow regimes. Overall, the results highlight the complex relationship between rod spacing, middle rod presence, and flow characteristics.

CONFLICT OF INTEREST

The author declares no conflict of interest.

DATA AVAILABILITY SOURCE

The data used in present study is available with corresponding author can be provided on reasonable request.

COMPETING INTEREST

The authors have no competing interest.

REFERENCES

1. Kolar, V., Lyn, D. A., Rodi, W. Ensemble-averaged measurements in the turbulent near wake of two side-by-side square rods. *Journal of Fluid Mechanics*. 346, 201-237. 1997.
2. Sumner, D., Wong, S. S. T., Price, S. J., Paidoussis, M. P. Fluid behaviour of side-by-side circular rods in steady cross-flow. *Journal of Fluids and Structures*. 13, 309–339. 1999.
3. Guillaume, D. W., LaRue, J. C. Investigation of the flopping regime with two-three- and four-rod arrays. *Experiments in Fluids*. 27, 145-156. 1999.
4. Zhang, H. J., Zhou, Y. Effect of unequal gap spacing on vortex street behind three side-by-side rods. *Physics of Fluids*. 13, 3675-3686. 2001.
5. Agrawal, A., Djenidi, L., Antonia, R. A. Investigation of flow around of a pair of side-by-side square rods using the lattice Boltzmann method. *Computers & Fluids*. 35, 1093-1107. 2006.
6. Chiu, A. Y. W., Ko, N. W. M. Bistable flows of two unequal square rods in various staggered arrangement. *Proceeding of the 12th Australian Fluid Mechanics Conference*. University of Sydney. 839-843. 1995.
7. Ma, S. C. W., Lim, T. B. A., Wu, C. H.,Tutty, O. Wake of two side-by-side square rods at low Reynolds numbers. *Physics of Fluids*. 29(3), 03304. 2017.
8. [8]Inoue, O., Iwakami, W., Hatakeyama, N. Aeolian tones radiated from flow past two square rods in a side-by-side arrangement. *Physics of Fluids*. 18, 046104, (1-20). 2006.
9. Islam, S. UL., Rahman, H., Zhou, C. Y., Saha, S. C. Comparison of wake structures and force measurements behind three side-by-side square rods. *Journal of the Brazilian Society of Mechanical Sciences and Engineering*. 38(3), 843–858. 2016.
10. Zdravkovich, M. M. Smoke observation of the wake of a group of three-rods at low Reynolds number. *J. Fluid Mech*. 32, 339-351.1968.
11. Zheng, Q. Intrinsic features of flow past three square prisms in side-by-side arrangement. *Journal of Fluid Mechanics*. 82, 996 – 1033. 2017.
12. Inoue, O., Suzuki, Y. Beat of sound generated by flow past three side-by-side square rods. *Physics of Fluids*. 19, 048102(1-4). 2007.
13. Burattini, P., Agrawal, A. Wake interaction between two side-by-side square rods in channel flow. *Computers & Fluids*. 77, 134–142. 2013.
14. Kang, S. Numerical study on laminar flow over three side-by-side rods. *KSME International Journal*. 18(10), 1869-1879. 2004.
15. Verma, P. L., Goverdhan, M. Flow behind bluff bodies in side-by-side arrangement. *Journal of Engineering Science and Technology*. 6(6), 745–768. 2011.
16. Rahman, H., Islam, S. UL., Zhou, C. Y., Kiyani, T., Saha, S. C. On the effect of Reynolds numbers for flow past three side-by-side square rods for unequal gap spacing's. *KSCE Journal of Civil Engineering*. 19(1), 233–247. 2014.
17. Wang, Z. J., Zhou, Y. Vortex interaction in a two side-by-side rod near wake. *International Journal of Heat and Fluid Flow*. 26(3), 362–377. 2005.
18. Han, Z., Zhou, D., Tu, J. Laminar flow patterns around three side-by-side arranged circular rods using semi-implicit three steps Taylor-characteristic-based-split (3-TCBS) algorithm. *Engineering Applications of Computational Fluid Mechanics*. 7, 1-12. 2013.
19. Guo, Z., Liu, H., Luo, L.-S., Xu, K. A comparative study of the LBE and GKS methods for 2D near incompressible laminar flows. *Journal of Computational Physics*. 227, 4955-4976. 2008.
20. Zhou, C. Y., Wang, L., Huang, W. Numerical study of fluid force reduction on a circular rod using tripping rods. *J. Mech. Sci. Tech*, 21, 1425-1435. 2009.
21. Yu, D., Mei, R., Luo, L. S., Shyy, W. Viscous flow computations with the method of lattice Boltzmann equation. *Progress in Aerospace Sciences*. 39(5), 329-367. 2003.
22. Frisch, U., Hasslacher, B., Pomeau, Y. Lattice gas automata for the Navier-Stokes equations. *Phys Rev Lett*. 56, 1505-8. 1986.
23. Breuer, M., Bernsdorf, J., Zeiser, T., Durst, F. Accurate computations of the laminar flow past a square rod based on two different methods: lattice-Boltzmann and finite-volume. *International journal of heat and fluid flow*. 21(2), 186-196. 2000.

24. Sumner, D., Wong, S. S. T., Price, S. J., Paidoussis, M. P. Fluid behaviour of side-by-side circular rods in steady cross-flow. *Journal of Fluids and Structures*. 13(3), 309-338. 1999.
25. Chatterjee, D., Biswas, G., Amiroudine, S. Numerical investigation of forced convection heat transfer in unsteady flow pasta row of square rods. *International journal of heat and fluid flow*. 30(6), 1114 – 1128. 2009.
26. Robichaux, J., Balachandar, S., Vanka, S. P. Two-dimensional Floquet instability of the wake of square rod. *Phys. Fluids*. 11, 560–578. 1999.
27. Sharma, A., Eswaran, V. Heat and fluid forces across a square rod in the two-dimensional laminar flow regime. *Numerical Heat Transfer. Part A: Applications*. 45(3), 247 – 269. 2004.